Drug Design Hot Paper

DOI: 10.1002/anie.201403936

Tumor-Targeting of EGFR Inhibitors by Hypoxia-Mediated Activation**

Claudia Karnthaler-Benbakka, Diana Groza, Kushtrim Kryeziu, Verena Pichler, Alexander Roller, Walter Berger, Petra Heffeter, and Christian R. Kowol**

Abstract: *The development of receptor tyrosine-kinase inhibitors (TKIs) was a major step forward in cancer treatment. However, the therapy with TKIs is limited by strong side effects and drug resistance. The aim of this study was the design of novel epidermal growth factor receptor (EGFR) inhibitors that are specifically activated in malignant tissue. Thus, a Co^{III}-based prodrug strategy for the targeted release of an EGFR inhibitor triggered by hypoxia in the solid tumor was used. New inhibitors with chelating moieties were prepared and tested for their EGFR-inhibitory potential. The most promising candidate was coupled to Co^{III} and the biological activity tested in cell culture. Indeed, hypoxic activation and subsequent EGFR inhibition was proven. Finally, the compound was tested in vivo, also revealing potent anticancer activity.*

Tyrosine kinases play a key role in human signal transduction processes, leading to cell growth and differentiation. Recent advances have implicated their role in the pathophysiology of cancer.[1] For example, overexpression of the epidermal growth factor receptor (EGFR, erbB1), a receptor tyrosine kinase, has been observed in a wide range of solid tumors, including those of head and neck, lung, colon, ovary, and breast, and has frequently been linked to a poor prognosis.[2] Thus, inhibition of the EGFR has emerged as an attractive strategy in anticancer drug research. A large number of small-molecule inhibitors has been developed, with 4-anilinoquinazolines as the most potent representatives.[3] Among them, the EGFR inhibitors gefitinib (Iressa) and erlotinib (Tarceva; Figure 1) were the first to be approved in 2003 and 2004, respectively, for the treatment of locally advanced or metastatic non-small-cell lung carcinoma (NSCLC) with activating EGFR mutations.[2] Additionally, erlotinib has been approved as first-line treatment of metastatic pancreatic cancer in combination with gemcitabine.[4] However, despite the benefits of EGFR tyrosine-kinase inhibitors (TKIs) and their increasing clinical use, drug-resistance development, insufficient tumor accumulation, and the occurrence of severe side effects, such as papulopustular skin rash, are major limitations for successful treatment.[5]

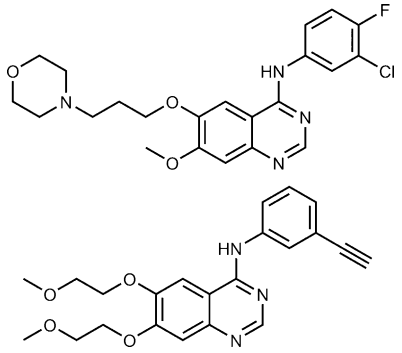

Figure 1. Chemical structures of gefitinib (Iressa; top) and erlotinib (Tarceva; bottom).

One promising approach to reduce the adverse effects of anticancer agents is to increase tumor selectivity by the use of prodrug systems. This concept is based on nontoxic compounds which release the corresponding active drugs only after specific activation in cancerous tissues.[6] For prodrug activation several cancer-targeting mechanisms have been reported, one of which being activation by reduction in the inherently hypoxic tissue found in most solid tumors.[7] This concept is of additional interest, since especially tumor cells that grow under anaerobic conditions develop resistance to chemotherapeutic agents.[8]

Cobalt(III) compounds can be used as such bioreducible prodrugs due to the Co^{III}/Co^{II} redox potential, which can be tuned to the range of cellular reductants,[8,9] and the significant difference in the ligand lability of the two oxidation states.[10] While octahedral d^6 low-spin Co^{III} complexes are kinetically inert, labile d^7 high-spin complexes are formed after reduction.[9a] In the absence of oxygen, which would immediately lead to re-oxidation, Co^{II} complexes easily

[*] M. Sc. C. Karnthaler-Benbakka,[+] Dr. V. Pichler, Dipl.-Ing. A. Roller, Dr. C. R. Kowol
Institute of Inorganic Chemistry, University of Vienna
Waehringer Strasse 42, 1090 Vienna (Austria)
E-mail: christian.kowol@univie.ac.at
M. Sc. D. Groza,[+] Mag. K. Kryeziu, Prof. Dr. W. Berger, Dr. P. Heffeter
Institute of Cancer Research, Medical University of Vienna
Borschkegasse 8A, 1090 Vienna (Austria)
E-mail: petra.heffeter@meduniwien.ac.at
Prof. Dr. W. Berger, Dr. P. Heffeter, Dr. C. R. Kowol
Research Platform "Translational Cancer Therapy Research"
University of Vienna and Medical University of Vienna
Vienna (Austria)
[+] These authors contributed equally to this work.

[**] This work was supported by the Fonds der Stadt Wien für innovative interdisziplinaere Krebsforschung, the FWF (P26603), and the COST action CM1105. We thank Prof. Mag. Dr. Walter Weissensteiner, University of Vienna, for helpful discussions. The authors declare a conflict of interest, as the lead compound is covered by a patent application.

Supporting information for this article is available on the WWW under http://dx.doi.org/10.1002/anie.201403936.

 © 2014 Wiley-VCH Verlag GmbH & Co. KGaA, Weinheim

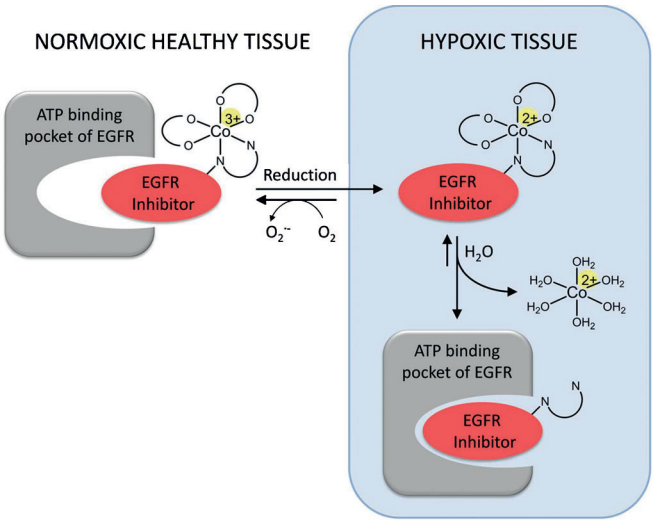

Figure 2. Schematic overview of the TKI Co^{III}-prodrug concept.

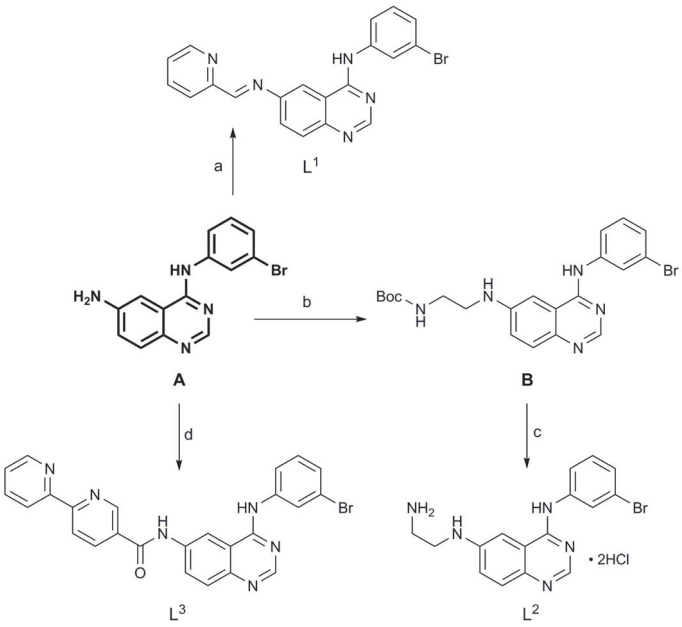

Scheme 1. Synthesis of L^1, L^2, and L^3. Reaction conditions: a) pyridine-2-carboxaldehyde, MeOH, reflux, 94%; b) *N*-Boc-2-aminoacetaldehyde, abs. MeOH, HOAc, molecular sieves (3–4 Å), then $NaBH_3CN$, 85%; c) conc. HCl, EtOH, reflux, 82%; d) 2,2′-bipyridine-5-carboxylic acid, HOBt·H_2O, TBTU, DIPEA, DMF, 60%. Boc = *tert*-butoxycarbonyl, DIPEA = *N*,*N*-diisopropylethylamine, HOBt = 1-hydroxy-1*H*-benzotriazole, TBTU = *O*-(benzotriazol-1-yl)-*N*,*N*,*N*′,*N*′-tetramethyluronium tetrafluoroborate.

undergo ligand substitution, enabling the selective release of biologically active ligands[10] (Figure 2). This concept has already been used for several cytotoxic compounds, such as nitrogen mustards[9a] and DNA intercalators.[11] However, despite their severe side effects, for the huge class of TKIs hardly any attempts concerning prodrug systems have been reported so far.[12] Thus, the aim of this work was the development of selectively hypoxia-activated EGFR inhibitors using Co^{III} complexes. This prodrug strategy is based on the assumption that the intact complexes would be too bulky and, therefore, prevent binding of the inhibitor to the ATP-binding pocket of the EGFR molecule. This enables the selective activity of the drug only after reduction and release in the hypoxic tumor tissue (Figure 2), resulting in reduced systemic toxicity, for example in the skin.

According to the literature, Co^{III} complexes with monodentate ligands lack selectivity for hypoxic cells.[9a] Thus, in this work, potential EGFR inhibitors with a bidentate chelating unit were synthesized. As the core structure, the 4-anilinoquinazoline moiety of the preclinically investigated inhibitor EKI-785 (CL-387,785)[13] was used. This moiety contains an NH_2 function at the 6-position of the quinazoline ring which is easily accessible for chemical modifications. As bidentate scaffolds, 2-pyridinemethanimine (L^1), ethylenediamine (L^2), and 2,2′-bipyridine (L^3) (Scheme 1) were selected. These moieties differ in their size and electronic properties such that their impact on the receptor binding ability could be investigated.

The core structure **A** was obtained by a three-step procedure according to Tsou et al.[14] L^1 was synthesized according to a modified literature procedure[15] using **A** and an excess of pyridine-2-carboxaldehyde in boiling methanol in 94% yield. L^2 was obtained by direct reductive amination of *N*-Boc-2-aminoacetaldehyde with **A** under slightly acidic conditions and sodium cyanoborohydride as the reducing agent, followed by deprotection using hydrochloric acid in an overall yield of 70%. L^3 was synthesized by coupling 2,2′-bipyridine-5-carboxylic acid and **A** using HOBt/TBTU in DMF.

In order to investigate whether the introduction of the chelating moiety interferes with their EGFR-inhibitory potential L^1, L^2, and L^3 were tested and compared to the known EGFR inhibitor erlotinib. As a first step, MTT assays were performed in wild-type EGFR-overexpressing erlotinib-sensitive A431 and Calu3 cells as well as in H1975 cells which harbor the erlotinib-resistance-conferring EGFR mutation T790M; the data were compared with the in vitro kinase inhibitory potential of the drugs (Table 1 and Figure S1). The bipyridyl-containing compound L^3 displayed the lowest activity with IC_{50} values far above 25 μM in all cell lines. Also due to the 2-pyridinemethanimine moiety, the anticancer activity of L^1 was distinctly lower than that of erlotinib, especially in A431 cells. Only in Calu3 cells activity in the low μM range was observed. In contrast, L^2, which contains the smallest chelating moiety, had IC_{50} values in the low μM range in both erlotinib-responsive models corresponding to the highest kinase inhibitory potential. Moreover, distinct activity

Table 1: Anticancer activity (72 h) and EGFR inhibitory potential.

Compound	Inhibition of cell growth [IC_{50} μM] A431	Calu3	H1975	EGFR inhibition [IC_{50}, nM]
erlotinib	2.6 ± 0.8	0.74 ± 0.02	> 25	2[17]
L^1	> 25	3.5 ± 0.1	20 ± 4	1.34
L^2	9.2 ± 0.5	2.0 ± 0.5	15 ± 2	0.95
L^3	> 25	> 25	> 25	4.59

© 2014 Wiley-VCH Verlag GmbH & Co. KGaA, Weinheim

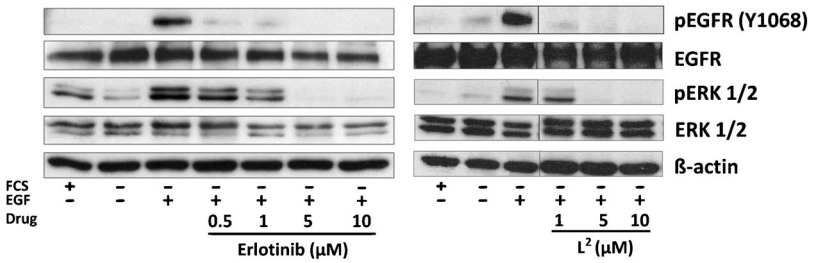

Figure 3. Inhibitory effects of L^2 and erlotinib on EGFR signaling. A431 cells were grown in medium with (+) or without (−) FCS and treated with the indicated drug for 4 h. After EGFR stimulation with 50 ng mL^{-1} EGF for 15 min, cells were harvested and lysed, and the activation of EGFR downstream pathways (pERK, pEGFR) was analyzed by Western blotting.

against erlotinib-resistant H1975 cells was observed with this ethylenediamine-containing ligand.

To verify that the effect of L^2 is based on inhibition of the EGFR signaling pathway also in the living cell, the impact of the novel drug on the EGFR-stimulated phosphorylation of EGFR and its downstream target ERK1/2 in A431 cells was analyzed by Western blotting (Figure 3). After 4 h of drug incubation the tested compounds showed dose-dependent inhibitory effects. These data indicate that L^2 is a potent EGFR inhibitor with an activity similar to that of erlotinib. Thus, L^2 was chosen for further development and complexation to Co^{III}.

As a Co^{III} precursor for the complexation of L^2, Na[Co(acac)$_2$(NO$_2$)$_2$] (**D**; acac = acetylacetonate) was used. This complex has been shown to undergo relatively rapid substitution of the two nitro groups with N,N-chelating systems.[9a,16] Complex **D** was synthesized from sodium hexanitrocobaltate(III) (**C**), which was treated with an aqueous solution of acetylacetone and sodium hydroxide.[18] Co^{III} complexes of L^2 were prepared in analogy to the method described by Ware et al.[9a] in the presence of activated charcoal using a mixture of water and methanol as the solvent (Figure 4A). Complex **1a** was obtained by precipitation with ammonium hexafluorophosphate and was purified by reversed-phase HPLC. The ^{1}H NMR spectrum of **1a** (Figure S2) showed two signal sets indicating the presence of two pairs of diastereomers due to the propeller chirality of the complex and the newly formed stereogenic center at the NH group of the ethylenediamine moiety. Slow crystallization with sodium perchlorate after acidification yielded only one isomeric form of the protonated perchlorate salt [**1**·HClO$_4$]ClO$_4$ (Figure 4B) as shown by X-ray crystallography.[19] After dissolution of the single crystals this isomer slowly interconverted again resulting in two signal sets in the ^{1}H NMR spectrum and preventing the isolation of pure diastereomers. Noteworthy, the metal-free ligand L^2 shows intrinsic fluorescence with a maximum at 455 nm when irradiated at 370 nm; this fluorescence is completely quenched by coordination to Co^{III} in complex **1a** (Figure 4C). Thus, the stability of **1a** in DMEM (Dulbecco's Modified Eagle Medium) could be analyzed by fluorescence spectroscopy and no significant release of ligand L^2 was observed during a period of 24 h. In addition, this feature also enabled the investigation of the hypoxia-mediated ligand release of **1a** by fluorescence microscopy.

Figure 5 shows the strong intracellular fluorescence of L^2 under normoxic and hypoxic conditions. In contrast, fluorescence in **1a**-treated cells was strongly diminished in normoxia, suggesting an intact Co^{III} complex. Under hypoxic conditions, a strong increase of fluorescence in **1a**-treated cells was detected, indicating activation of the prodrug with subsequent ligand release.

Next, the anticancer activity of the novel Co^{III} complex was compared to that of the metal-free ligand under normoxic and hypoxic conditions (see Figure 6, Figure S3, and Figure S4A). Complex **1a** was widely inactive under normoxic conditions (up to

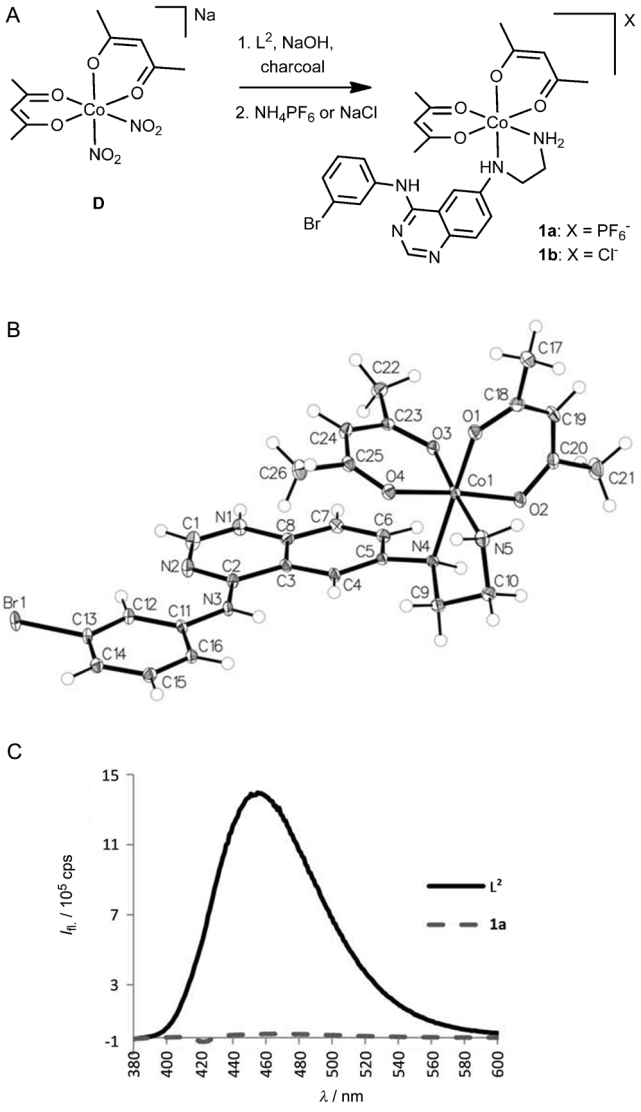

Figure 4. A) Synthesis of complexes **1a** and **1b**. B) X-ray crystal structure of [**1**·HClO$_4$]ClO$_4$; atomic displacement ellipsoids set at 50% probability; counter ions omitted for clarity). C) Fluorescence emission spectra of 30 μM solutions of L^2 and **1a** in phosphate-buffered saline.

 © 2014 Wiley-VCH Verlag GmbH & Co. KGaA, Weinheim

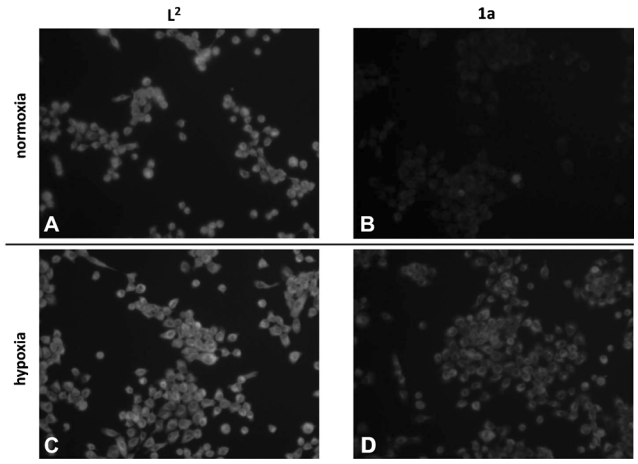

Figure 5. Ligand release of **1a** upon hypoxic activation observed in comparison to L^2 using UV fluorescence microscopy. A431 cells were incubated with 10 μM L^2 (A and C) and **1a** (B and D) under normoxic (A and B) and hypoxic (C and D) conditions, respectively, for 6 h.

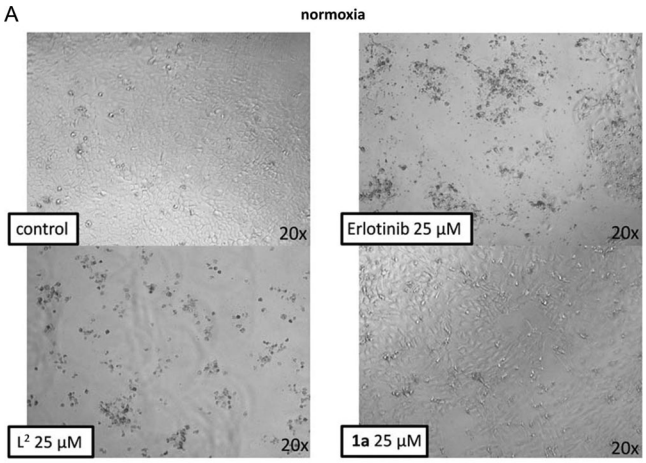

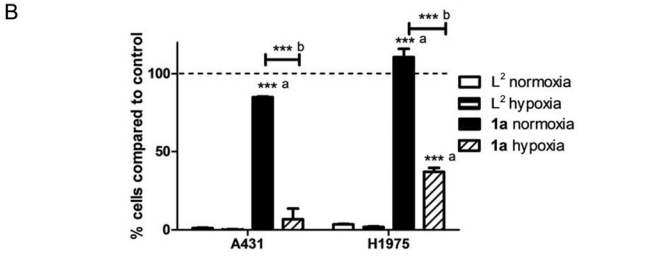

Figure 6. Impact of hypoxia on the anticancer activity of erlotinib, L^2, and **1a**. A) A431 cells were treated with L^2, **1a**, and erlotinib under normoxic conditions for 72 h. B) A431 (EGFR-overexpressing) and H1975 (overexpression of EGFR with an activating L858R and the secondary T790M resistance mutation) were incubated with 25 μM L^2 or **1a** under hypoxia or normoxia for 72 h. Cell viability was measured using a MTT-based system. Values given are means ± standard deviation (SD) of one representative experiment performed in triplicate (Statistical analysis: t-test; ***$p < 0.001$; a: difference between L^2 and **1a**; b: difference between **1a** normoxia and **1a** hypoxia).

the highest tested concentration of 25 μM). In contrast, when cells were treated under hypoxia, the activity of **1a** was significantly increased. As expected, the potent anticancer activity of L^2 was only marginally influenced by hypoxia. Notably, comparable cobalt complexes without any EGFR-inhibiting moiety (i.e. $[Co^{II}(acac)_2en]$ (en = ethylenediamine) and $[Co^{III}(acac)_2en]PF_6$) had no significant activity (Figure S4B), thus excluding a major contribution of the cobalt core itself.

In accordance with the viability assays, Western blot analysis revealed that also the EGFR-inhibitory potential of **1a** was distinctly reduced under normoxic conditions, while potent activity similar to that of the metal-free ligand L^2 was found under hypoxia (Figure 7 and Figure S5). Altogether, these experiments indicate that the complexation of L^2 to Co^{III} efficiently hampers receptor binding and EGFR inhibition under normoxic conditions, while hypoxia leads to ligand release and potent activity against EGFR-driven cancer cells in vitro.

Thus, the activity of the new drug was tested against EGFR-driven xenografts in SCID mice. For this purpose, the better water soluble chloride salt **1b** was prepared by precipitation of the complex with brine and purified further by reversed-phase HPLC (Figure 4A, identical cytotoxic activity of **1a** and **1b** was checked in several cell lines by MTT assay (data not shown)). In general, treatment with **1b** was well tolerated even after repeated applications either intraperitoneally or via the tail vein. With regard to its anticancer activity, **1b** potently inhibited tumor growth of A431 xenografts with an efficacy comparable to that of erlotinib (especially upon intraperitoneal application; Figure 8). Notably, in Calu3 xenografts **1b** repeatedly induced distinct tumor regression when a tumor size of more than 200 mm^3 was reached (in contrast to resistance development during later therapy cycles in the case of erlotinib as shown in Figure 8D). This response to **1b** treatment is of special interest, as Calu3 xenografts are characterized by a rather specific tumor histology where small tumor islands are

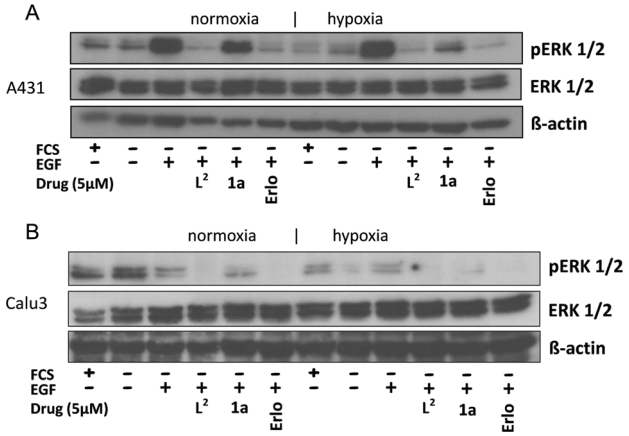

Figure 7. Impact of hypoxia on the EGFR-inhibitory potential of L^2, **1a**, and erlotinib. A) A431 and B) Calu3 cells were grown in medium with (+) or without (−) FCS and treated with 5 μM of the indicated drugs for 4 h. After EGFR stimulation with 50 ng mL^{-1} EGF for 15 min, the cells were harvested and lysed, and the phosphorylation levels of ERK1/2 as well as total ERK1/2 were determined by Western blotting. The respective EGFR blots are shown in Figure S5A.

 © 2014 Wiley-VCH Verlag GmbH & Co. KGaA, Weinheim

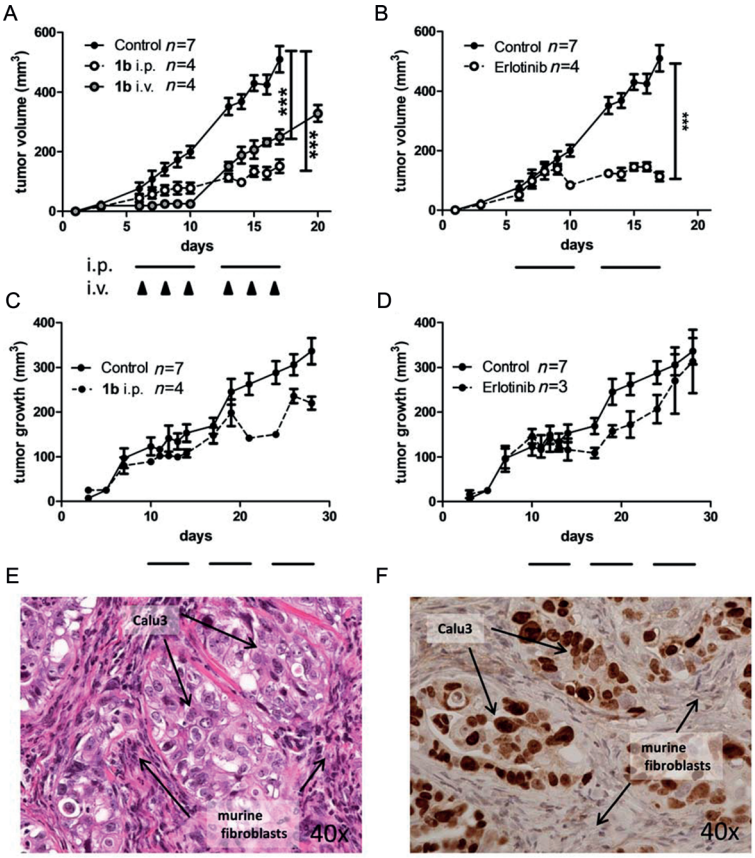

Figure 8. In vivo anticancer activity of **1b** and erlotinib in xenografts with human cancer cells. A431 (A, B) and Calu3 (C, D) were injected subcutaneously into the right flank of CB-17/SCID mice. When tumors were palpable, **1b** was given as indicated. The applied dose was 5 mg kg^{-1} for i.v. and 25 mg kg^{-1} for i.p. application, respectively. Erlotinib was given at 25 mg kg^{-1} orally. For i.p. and oral therapy, cycles of five consecutive days are indicated by black bars, days of i.v. treatment are indicated by black arrows. Tumor volumes were calculated as described in the experimental section (Supporting Information). Data are means +/− SEM. Statistical significance tests: two-way ANOVA (*** $p < 0.001$). On the last day of treatment the tumors were collected and histologically processed. Tissue morphology of untreated Calu3 xenografts was analyzed by E) H&E-stain and F) immunostain for human Ki67.

surrounded by murine fibroblasts (Figure 8E,F). Consequently, in these xenografts a larger tumor volume seems to be necessary for the development of hypoxic conditions and, thus, activation of **1b.** Notably, to the best of our knowledge, this is the first proof of the in vivo anticancer activity of a hypoxia-activatable Co^{III} complex.

Taken together, the occurrence of severe side effects (such as skin rash) based on tyrosine-kinase inhibition in healthy tissue is among the major limitations of EGFR inhibitors. Thus, there is urgent need for the development of tumor-specifically activated prodrugs. Hypoxia targeting represents a compelling strategy to achieve this goal,[7] especially as hypoxia plays a major role in tumor development and resistance to therapy, and since hypoxic tumors are known for their poor prognosis.[7c,20]

Based on these facts, several attempts have already been made to activate cytotoxic drugs by hypoxic conditions and some substances are currently successfully tested in clinical phase II and III trials.[7b] In this study such an activating strategy has been successfully applied for the first time for tyrosine-kinase inhibitors using a Co^{III} prodrug design with a novel EGFR inhibitor possessing a bis-chelating moiety. Subsequent analysis revealed the hypoxia-activatable properties of this new complex and potent anticancer activity against EGFR-driven cancer cells in cell culture and in vivo. Summarizing, our study shows that Co^{III}-based tumor-targeting represents a promising strategy to improve EGFR inhibitor therapy.

Received: April 2, 2014
Published online: July 30, 2014

Keywords: anticancer drugs · cobalt · hypoxia · prodrugs · tyrosine-kinase inhibitors

[1] M. K. Paul, A. K. Mukhopadhyay, *Int. J. Med. Sci.* **2004**, *1*, 101 – 115.
[2] S. V. Sharma, D. W. Bell, J. Settleman, D. A. Haber, *Nat. Rev. Cancer* **2007**, *7*, 169 – 181.
[3] V. Chandregowda, A. K. Kush, G. C. Reddy, *Eur. J. Med. Chem.* **2009**, *44*, 3046 – 3055.
[4] C. M. Rocha-Lima, H. P. Soares, L. E. Raez, R. Singal, *Cancer Control* **2007**, *14*, 295 – 304.
[5] a) G. Lurje, H. J. Lenz, *Oncology* **2009**, *77*, 400 – 410; b) T. Li, R. Perez-Soler, *Targ. Oncol.* **2009**, *4*, 107 – 119.
[6] I. Tranoy-Opalinski, A. Fernandes, M. Thomas, J. P. Gesson, S. Papot, *Anticancer Agents Med. Chem.* **2008**, *8*, 618 – 637.
[7] a) M. A. Naylor, P. Thomson, *Mini-Rev. Med. Chem.* **2001**, *1*, 17 – 29; b) W. R. Wilson, M. P. Hay, *Nat. Rev. Cancer* **2011**, *11*, 393 – 410; c) J. M. Brown, W. R. William, *Nat. Rev. Cancer* **2004**, *4*, 437 – 447.
[8] I. Ott, R. Gust, *Arch. Pharm.* **2007**, *340*, 117 – 126.
[9] a) D. C. Ware, B. D. Palmer, W. R. Wilson, W. A. Denny, *J. Med. Chem.* **1993**, *36*, 1839 – 1846; b) U. Jungwirth, C. R. Kowol, B. K. Keppler, C. G. Hartinger, W. Berger, P. Heffeter, *Antioxid. Redox Signaling* **2011**, *15*, 1085 – 1127.
[10] M. C. Heffern, N. Yamamoto, R. J. Holbrook, A. L. Eckermann, T. J. Meade, *Curr. Opin. Chem. Biol.* **2013**, *17*, 189 – 196.
[11] a) G. O. Ahn, K. J. Botting, A. V. Patterson, D. C. Ware, M. Tercel, W. R. Wilson, *Biochem. Pharmacol.* **2006**, *71*, 1683 – 1694; b) J. Y. C. Chang, R. J. Stevenson, G. L. Lu, P. J. Brothers, G. R. Clark, W. A. Denny, D. C. Ware, *Dalton Trans.* **2010**, *39*, 11535 – 11550; c) J. B. Milbank, R. J. Stevenson, D. C. Ware, J. Y. C. Chang, M. Tercel, G. O. Ahn, W. R. Wilson, W. A. Denny, *J. Med. Chem.* **2009**, *52*, 6822 – 6834.
[12] D. Baiz, T. A. Pinder, S. Hassan, Y. Karpova, F. Salsbury, M. E. Welker, G. Kulik, *J. Med. Chem.* **2012**, *55*, 8038 – 8046.
[13] a) C. M. Discafani, M. L. Carroll, M. B. Floyd, Jr., I. J. Hollander, Z. Husain, B. D. Johnson, D. Kitchen, M. K. May, M. S. Malo, A. A. Minnick, Jr., R. Nilakantan, R. Shen, Y. F. Wang, A. Wissner, L. M. Greenberger, *Biochem. Pharmacol.* **1999**, *57*, 917 – 925; b) T. Barf, A. Kaptein, *J. Med. Chem.* **2012**, *55*, 6243 – 6262.
[14] H. R. Tsou, N. Mamuya, B. D. Johnson, M. F. Reich, B. C. Gruber, F. Ye, R. Nilakantan, R. Shen, C. Discafani, R. DeBlanc, R. Davis, F. E. Koehn, L. M. Greenberger, Y. F. Wang, A. Wissner, *J. Med. Chem.* **2001**, *44*, 2719 – 2734.

 © 2014 Wiley-VCH Verlag GmbH & Co. KGaA, Weinheim

[15] A. Bourkoula, M. Paravatou-Petsotas, A. Papadopoulos, I. Santos, H. J. Pietzsch, E. Livaniou, M. Pelecanou, M. Papadopoulos, I. Pirmettis, *Eur. J. Med. Chem.* **2009**, *44*, 4021 – 4027.
[16] R. D. Archer, B. P. Cotsoradis, *Inorg. Chem.* **1965**, *4*, 1584 – 1589.
[17] J. D. Moyer, E. G. Barbacci, K. K. Iwata, L. Arnold, B. Boman, A. Cunningham, C. DiOrio, J. Doty, M. J. Morin, M. P. Moyer, M. Neveu, V. A. Pollack, L. R. Pustilnik, M. M. Reynolds, D. Sloan, A. Theleman, P. Miller, *Cancer Res.* **1997**, *57*, 4838 – 4848.
[18] L. J. Boucher, J. C. Bailar, *J. Inorg. Nucl. Chem.* **1965**, *27*, 1093 – 1099.
[19] Crystal data for [**1**·$HClO_4$]ClO_4: $C_{26}H_{31}BrCl_2CoN_5O_{12}$, M_r = 815.30, crystal size = 0.040 × 0.049 × 0.312 mm, triclinic, *P*1, *a* = 7.7893(4), *b* = 12.3702(7), *c* = 16.7844(9) Å, *α* = 82.404(2), *β* = 78.264(2), *γ* = 76.685(2)°, *V* = 1534.70(14) Å^3, *Z* = 2, ρ_{calcd} = 1.764 g cm^{-3}, *μ* = 2.108 mm^{-1}, *λ*($Mo_{K\alpha}$) = 0.71073 Å, *T* = 100 K, $2\theta_{max}$ = 60.29°, 58928 reflections measured, 9022 unique (R_{int} = 0.0552), R_1 = 0.0500, wR_2 = 0.1269, largest difference peak and hole: 1.084 and −0.702 e A^{-3}. CCDC 994541 contains the supplementary crystallographic data for this paper. These data can be obtained free of charge from The Cambridge Crystallographic Data Centre via www.ccdc.cam.ac.uk/data_request/cif.
[20] Y. Wang, M. Ohh, *J. Cell. Mol. Med.* **2010**, *14*, 496 – 503.

 © 2014 Wiley-VCH Verlag GmbH & Co. KGaA, Weinheim